anteromedial corner. Azimuths between $20°_c$ and 0° were disproportionately well represented, but azimuths beyond $30°_c$ and $10°_i$ received little representation.

Sound elevation was arranged dorsoventrally in the transverse plane: high best areas were located dorsally; low best areas were located ventrally. Best-area centers ranged in elevation from +20° to −90° with greatest representation given to the area between −10° and −60°.

This map of auditory space is an emergent property of higher-order neurons, distinguishing it from all other sensory maps that are direct projections of the sensory surface. The auditory system must derive its map from the relative patterns of auditory nerve input arriving from the two ears. This requires that (i) there exist unique interaural intensity or time criteria for each area of auditory space, (ii) the auditory input be connected in such a way that each central neuron responds to a slightly different set of criteria corresponding to a slightly different area of space (*18*), and (iii) these neurons be arranged so that the order of their receptive fields conforms to the continuity of auditory space. Because these space-related response properties and functional organization must be specifically generated through neuronal integration by the central nervous system, it seems likely that these neurons in this specialized region of the midbrain are intimately involved in the analysis of spatial aspects of auditory signals.

ERIC I. KNUDSEN
MASAKAZU KONISHI

Beckman Laboratories of Behavioral Biology, California Institute of Technology, Pasadena 91125

References and Notes

1. G. von Békésy, *Experiments in Hearing*, E. G. Wever, Transl. and Ed. (McGraw-Hill, New York, 1960). The theory was later expanded by W. A. van Bergeijk [*J. Acoust. Soc. Am.* **34**, 1431 (1962)].
2. L. A. Jeffress, *J. Comp. Physiol. Psychol.* **41**, 35 (1948).
3. For a review of neurophysiological studies on sound localization, see S. D. Erulkar, *Physiol. Rev.* **52**, 237 (1972).
4. J. L. Hall, *J. Acoust. Soc. Am.* **37**, 814 (1965); F. Flammino and B. M. Clopton, *ibid.* **57**, 692 (1975); A. Starr, *Fed. Proc. Fed. Am. Soc. Exp. Biol.* **33**, 1911 (1974).
5. E. I. Knudsen, M. Konishi, J. D. Pettigrew, *Science* **198**, 1278 (1977); B. Gordon, *Sci. Am.* **227**, 72 (December 1972); F. Morrell, *Nature (London)* **238**, 44 (1972); B. G. Wickelgren, *Science* **173**, 69 (1971); E. I. Evans, in *Ciba Foundation Symposium on Hearing Mechanisms in Vertebrates* (Churchill, London, 1968).
6. By analogy to its connotation in contemporary visual research, the term "receptive field" will refer to the area of space within which a sound stimulus can influence the firing of an auditory neuron.
7. The anechoic chamber measured 3 by 3 by 5 m and was free of standing waves due to reflection for the frequency range used; sound attenuation followed the inverse-square law.
8. The speaker (5 cm) was calibrated with a 2.5-cm condenser microphone (Bruel & Kjaer) placed at the position where the owl would be located. The frequency response of the speaker was flat from 4 to 10 kHz. Variation in sound intensity as a function of speaker location was less than ±2 dB except in a small area directly beneath the owl.
9. The speaker moved in azimuth along a semicircular track 2 cm wide and 2 m in diameter. The track could be rotated to provide changes in speaker elevation. Azimuth and elevation were controlled independently by two stepping motors located outside the chamber. Thus the speaker could be positioned at any point on a sphere of radius 1 m centered at the owl's head, except for a 20° sector blocked by a supporting post for the owl.
10. The highly pigmented pecten oculi in each eye, which is plainly visible ophthalmoscopically, provided a convenient landmark for aligning the owl's head. The visual plane is the horizontal plane containing the projection from each area centralis through the nodal point of the eye to the horizon. In the barn owl the visual plane is located 8° to 10° below the plane containing the projections of the superior limbs of each pecten into space. The owl's visual plane was adjusted by monitoring the projection angle of the superior limbs of the pectens. Medial plane alignment was achieved by positioning the owl so that its pectens projected symmetrically on either side of the 0° azimuth plane.
11. Noise and tone bursts were 100 msec in duration with 2.5-msec rise and decay times and were repeated at a rate of 0.75 to 1 per second. The noise spectrum was 1 to 10 kHz, and the click spectrum predominately 4 to 8 kHz.
12. Units were tested for sensitivity to visual stimuli by sweeping bars and spots of light across a tangent screen temporarily placed 57 cm in front of the owl. The screen was removed during acoustic stimulation. The MLD units were not responsive to visual stimulation.
13. H. J. Karten, *Brain Res.* **6**, 409 (1967).
14. Units were recorded extracellularly with glass-insulated tungsten electrodes. The electrode penetration angle was 45° to the ear canal–beak hinge axis (that is, in the transverse plane) as measured by a protractor.
15. M. Konishi, *Am. Sci.* **61**, 414 (1973).
16. Unit thresholds ranged from −10 to +36 dB sound-pressure level.
17. We have adopted the conventions of H. J. Karten and W. Hodos [*A Stereotaxic Atlas of the Brain of the Pigeon* (Columba livia) (Johns Hopkins Press, Baltimore, 1967)] in defining the planes of section.
18. Attenuation of sound intensity to one ear by earplugging severely altered the receptive fields of these midbrain units.
19. We thank A. J. Hudspeth for critically reviewing the manuscript. This work was supported by an NIH postdoctoral fellowship 1 F32 NS 05529-01 to E.I.K.

6 September 1977; revised 14 December 1977

Intracellular Calcium: Its Movement During Pentylenetetrazole-Induced Bursting Activity

Abstract. *The intracellular calcium concentration in the cytoplasm decreased and the calcium concentration near the cell membrane increased during bursting activity induced by pentylenetetrazole in snail neuron. Incubation in medium containing cobalt chloride or lanthanum chloride did not change this tendency, which suggests that this calcium distribution change is due to the stored calcium in the subcellular structure moving toward the cell membrane.*

The cerebral cortical neuron of the cat shows a characteristic bursting firing pattern on injection of pentylenetetrazole (PTZ) (*1*). Some of the identifiable neurons of *Aplysia* and snails also respond to PTZ application with a characteristic bursting activity or sustained depolarization that strongly resembles the PTZ-induced change in the mammalian cerebral cortical neuron (*2*, *3*). This bursting activity is considered to be of endogenous origin, and these cells generally show negative resistance characteristics in voltage clamping experiments (*4*). Electrophysiological and neurochemical investigations (*5*) have indicated that calcium ion is very important for such bursting activity.

Because of the technical difficulties involved, however, little is known about the intracellular movement of calcium during bursting activity induced by PTZ. The electron probe x-ray microanalyzer (EPXMA) makes possible investigations of intracellular ionic movement in relation to the cellular ultrastructure. We discuss here the calcium and magnesium distribution changes induced by PTZ that are due to intracellular calcium movement.

Identifiable D neurons of the subesophageal ganglion of the Japanese land snail *Euhadra peliomphala* were used. These neurons are more sensitive to PTZ than are other types of neurons (*3*). The ganglia were dissected and divided into two groups, one of which was incubated in snail Ringer solution containing PTZ (5×10^{-2} mole) and the other in normal snail Ringer solution. After 15 minutes of incubation, both groups were dipped into Freon 12 cooled by liquid nitrogen. The Freon 12 was solid except for a small volume, which was melted by a copper block just before the specimens were dipped. The frozen ganglia were freeze-dried in a deep freezer (below −35°C) without passing through a liquid phase. The D neuron was easily picked up from the freeze-dried cluster by use of a fine forceps. Spot analysis of calcium and magnesium was performed.

For computer-controlled mapping of the calcium distribution, the ganglion was prepared so that the D neuron could easily be sectioned later in a freezing chamber. The ganglion was quickly removed, placed on an aluminum holder, and dipped in liquid Freon 12 as described above. A frozen thin section of

0036-8075/78/0519-0797$00.50/0 Copyright © 1978 AAAS

the D neuron about 10 μm thick was prepared with a Lipshaw freezing microtome, which had been modified for this purpose. The sample holder was cooled by liquid nitrogen. Thin-sectioned specimens were placed on a handmade carbon disk that had been precooled in a freezing chamber and were transferred, while cooled with liquid nitrogen, into a deep freezer, where they were freeze-dried without passing through a liquid phase. During this procedure no visible ice crystals were observed.

The freeze-dried specimens were placed on a carbon disk, which was fitted into the EPXMA sample stage. To keep the measuring conditions constant, the control and PTZ-treated specimens were put on the same carbon disk and their calcium distributions were measured successively at the same accelerating voltage (15 kV) and absorbed current (10^{-8} A). A JEOL 50A x-ray microanalyzer combined with a DEC-8 computer with an interface made by the Japan Electron Optic Laboratory was used. The language for EPXMA operation, called JECAS-X, was also prepared by the Japan Electron Optic Laboratory. Computer-controlled stepwise analysis was used for mapping of the ion distribution. Searching for the peak of the secondary x-ray intensity of calcium and magnesium was performed automatically and the exact crystal position was detected promptly. The analyzing spot was automatically advanced in 3-μm steps on the x-axis and 5-μm steps on the y-axis. The beam spot size was 4 μm in diameter, so that the analysis covered the whole surface of the specimen. During its stepwise movement, the electron beam was stopped with a beam shutter in order to minimize specimen damage. The analysis time was 10 seconds for one spot. The measured counts were classified in ten steps, from 0 to X.

Figure 1 shows the calcium and magnesium distributions in control and PTZ-treated neurons. The calcium density approximately doubled in PTZ-treated neu-

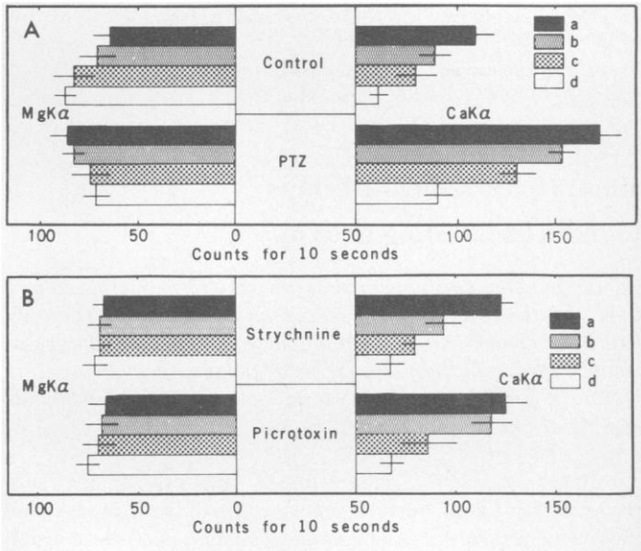

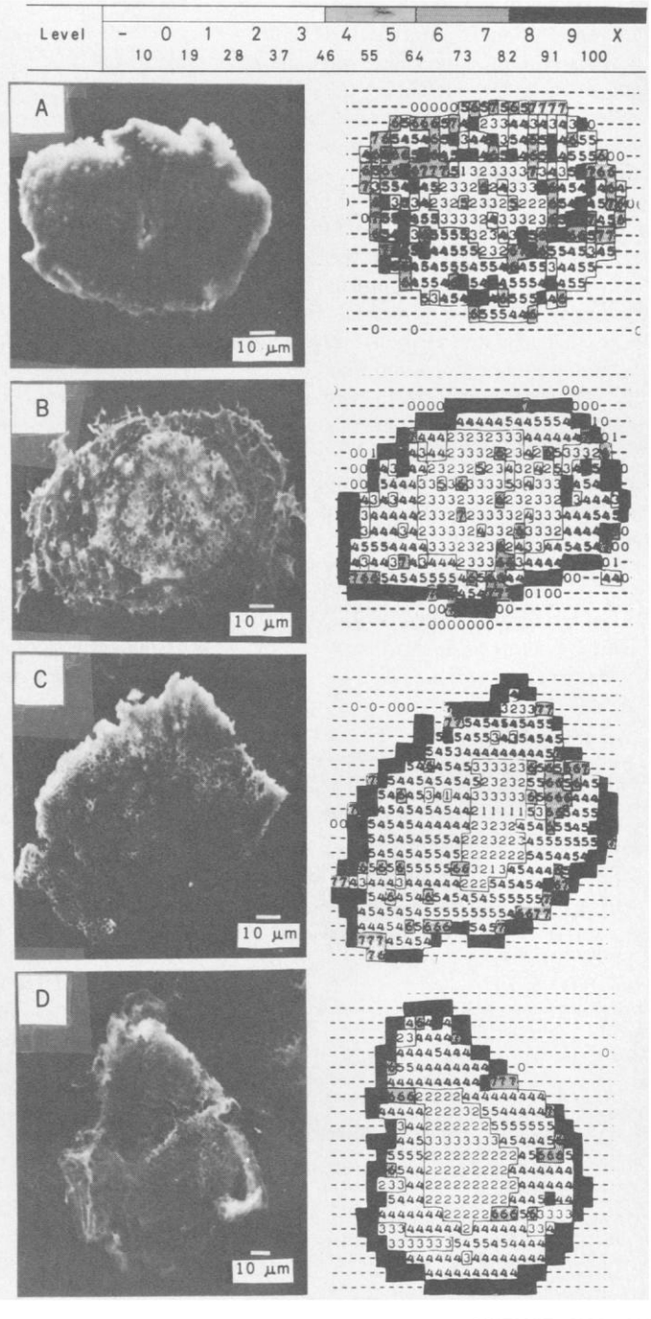

Fig. 1 (left). Effect of convulsants on the calcium and magnesium distributions in a single isolated snail neuron. The regions analyzed were (a) the axon hillock, (b) near the axon hillock, (c) far from the axon hillock, and (d) the cell body. (A) and (B) were obtained under the same conditions. Values are means ± standard deviations from six experiments. Fig. 2 (right). Intracellular calcium distribution changes induced in a D neuron by PTZ. Specimen preparation is described in the text. The photographs are secondary electron images of analyzed neurons; the maps were prepared by computer. Measured counts were classified in ten steps or levels, as shown at the top; the numbers in the maps correspond to these levels, except that levels of 8 or more are densely shaded in the maps. These results are for D neurons incubated in (A) normal Ringer solution, (B) PTZ Ringer solution, (C) PTZ Ringer solution with cobalt chloride, and (D) PTZ Ringer solution with lanthanum chloride.

rons, but the distribution pattern did not change. The magnesium distribution pattern was reversed by the application of PTZ; magnesium increased in the axon hillock region and decreased in the cell body. Convulsant drugs other than PTZ, such as strychnine (1×10^{-2} mole) and picrotoxin (5×10^{-3} mole), had little effect, as shown in Fig. 1B. Similarly, PTZ has the greatest effect and strychnine and picrotoxin have only a slight effect on intracellular potential change in the D neuron of *Euhadra*.

Figure 2 shows a more detailed general view of the distribution changes induced by PTZ. Calcium, which was concentrated in the cytoplasm in the normal state (Fig. 2A), became more concentrated in and near the cell membrane and less concentrated in the cytoplasm (Fig. 2B) on PTZ application.

In the *Euhadra* ganglion, the neurons can be classified into three types: D neurons, which are depolarized by acetylcholine (ACh); H neurons, which are hyperpolarized by ACh; and I neurons, which are indifferent to ACh (*3*). The I neurons are slightly depolarized by application of PTZ but never manifest bursting activity. We compared the I and D neurons with respect to calcium distribution changes induced by PTZ. The I neurons [RO-1 or LO-1 according to the classification in (*3*)] were incubated in normal or PTZ-containing Ringer solution, frozen, and thin-sectioned. Freeze-dried specimens of both samples were examined. The results showed that no intracellular calcium distribution change was induced by PTZ in the I neuron.

To determine the origin of the increased calcium more precisely—that is, whether it was extracellular or intracellular—the same procedures were carried out with solutions containing cobalt chloride or lanthanum chloride. Figure 2, C and D, show the maps obtained with PTZ Ringer solution containing 30 m*M* cobalt chloride and 4.5 m*M* lanthanum chloride, respectively. The calcium distribution pattern changes are almost the same as those observed with PTZ only. These results suggest that the calcium concentrated in or near the cell membrane on application of PTZ is mainly of intracellular origin.

In voltage clamping studies, the bursting cell shows negative resistance characteristics; this phenomenon is considered to be caused by influx of calcium (*6*). Calcium influx may occur during the bursting activity, but at the same time as or before it occurs the intracellular calcium, probably bound to some granule, to endoplasmic reticulum, or to mitochondria, is released and moves toward the cell membrane. Binding to the inner or outer surface of the cell membrane may then occur and trigger changes in ion channels, probably for potassium and sometimes for calcium. This could be the intracellular mechanism of PTZ-induced bursting activity. The EPXMA provides a promising technique for the study of intracellular ion movement in relation to ultrastructural changes.

EIICHI SUGAYA
MINORU ONOZUKA
Department of Physiology, Kanagawa Dental College, Yokosuka, Japan

References and Notes

1. E. Sugaya, S. Goldring, J. L. O'Leary, *Electroencephalogr. Clin. Neurophysiol.* **17**, 661 (1964).
2. N. Chalazonitis and H. Takeuchi, *C. R. Seances Soc. Biol. Paris* **162**, 1552 (1968); D. S. Faber and M. R. Klee, *Pfluegers Arch.* **332**, R66 (1972); E. U. Speckmann and H. Caspers, *Epilepsia* **14**, 397 (1973).
3. A. Sugaya *et al.*, *Jpn. J. Physiol.* **23**, 261 (1973).
4. M. R. Klee and D. S. Faber, *Science* **179**, 1133 (1973); R. J. David, W. A. Wilson, A. V. Escueta, *Brain Res.* **67**, 549 (1974); C. Ducreux and M. Gola, *Pfluegers Arch.* **361**, 43 (1975).
5. J. L. Barker and H. Gainer, *Brain Res.* **84**, 479 (1975).
6. R. Eckert and H. D. Lux, *J. Physiol. (London)* **254**, 129 (1976).
7. We thank S. Okudera and Y. Ono for help in computer programing. Supported in part by a grant from the Japanese Ministry of Education, Science and Culture.

14 October 1977

Dyskinesias Evoked in Monkeys by Weekly Administration of Haloperidol

Abstract. *In two cebus (*Cebus albifrons*) monkeys given weekly oral doses of 0.25 milligram of haloperidol per kilogram, movement disorders appeared 1 to 8 hours after drug administration following the tenth weekly dose. These disorders included oral movements, peculiar postures, writhing, and stretching. Such reactions faded in intensity after the next two doses. Increasing the dose to 0.5 milligram per kilogram has elicited the disorders reliably after each weekly dose for almost 2 years. Similar reactions also developed in a squirrel monkey (*Saimiri sciurea*) treated weekly with haloperidol and in a third cebus monkey previously maintained for a year on a regimen of 0.25 milligram of haloperidol per kilogram on 5 days per week. These findings suggest an experimental model for determining the etiology of drug-induced movement disorders. They also suggest an unrecognized clinical problem.*

Drug therapy dominates the psychiatric treatment of behavior disorders. Its efficacy is limited, however, by widespread pharmacologic mismanagement (*1*) and by the inherent toxicity of the drugs. These two factors are closely connected because the most prominent toxic manifestations are neurobehavioral, producing on the part of clinicians an understandable confusion between side effects and primary behavioral disturbances. Movement disorders represent the most salient and disturbing toxic reactions (*2*). Such disorders may develop as rapidly as a few hours after a single dose of a drug or develop only after years of treatment. Acute dyskinesias assume a variety of forms, including grimacing, yawning, abnormal tongue excursion, writhing motions of the trunk and limbs, and spasmodic, prolonged tonic contractions. Parkinsonism may occur after several weeks of treatment. Persistent or tardive dyskinesias resemble acute reactions in many ways except that oral-facial movements are more conspicuous, and the syndrome emerges after prolonged therapy. Sometimes it may even develop only after medication is halted or reduced (*3*). Although rarely mentioned, the frequency spectrum of resting finger tremor may also identify tardive dyskinesia (*4*). The tardive dyskinesias arouse the most concern because they develop insidiously, often seem to be irreversible, and, ironically, some-

Fig. 1. Monkey 39 after the tenth weekly dose of haloperidol (0.25 mg/kg). The hind legs remain straight, the forearms stretched backward parallel to the torso. (The tip of the paw lies under the inverted V. The V pointed sideways is aimed just below the elbow.) The open mouth is part of a yawn sequence that appeared several times per minute at its peak frequency.

0036-8075/78/0519-0799$00.50/0 Copyright © 1978 AAAS